

# Instrumented Harmonic Drives for Robotic Compliant Maneuvers

H. Kazerooni

Mechanical Engineering Department  
University of Minnesota, Minneapolis, MN 55455

## Abstract

Since torque in harmonic drives is transmitted by a pure couple, harmonic drives do not generate radial forces and therefore can be instrumented with torque sensors without interference from radial forces. The installation of torque sensors on the stationary component of harmonic drives (the Flexipline cup in this research work) produce backdrivability needed for robotic compliant maneuvers [2]. This article first develops the dynamic behavior of a harmonic drive, in particular the non-backdrivability, in terms of a sensitivity transfer function (or 1/impedance) [5]. The instrumentation of the harmonic drive with torque sensor is then described. This leads to a description of the control algorithm which allows modulation of the sensitivity transfer function within the limits established by the closed-loop stability criteria. A set of experiments on an active hand controller, powered by a DC motor coupled to an instrumented harmonic drive, is given to verify the theoretical predictions.

## 1. Introduction

Developed over 30 years ago primarily for aerospace applications, harmonic drives are compact transmission systems which increase the torque of electric motors. Harmonic drives consist of three simple parts and thus offer practitioners the freedom to incorporate drive components into machines or equipment. This article first gives a summary of the harmonic drive's principle of operation. Section 3 discusses the dynamic behavior of the harmonic drive where it is shown that large reduction ratios (usually more than 60) result in non-backdrivable systems [2, 5]. This leads to a discussion of the sensors required to make the harmonic drive arbitrarily backdrivable. Section 4 develops the control technique that produces stable backdrivability in the system. Section 5 describes the trade-offs between the stability and performance. The theoretical predictions are verified in Section 6 via a set of experiments on an active hand controller.

## 2. Summary of the Principle of Operation

To describe the drive's principle of operation, we use its most common mode of operation: speed reducer.

Harmonic drives have three elements [1]: 1) *Elliptical Wave Generator*, 2) *Flexipline (or Cup)*, and 3) *Rigid Circular Spline* (Figure 1). The Elliptical Wave Generator is an elliptical bearing attached to the motor drive shaft. The Flexipline is a nonrigid cup whose inner surface grasps the Wave Generator at the cup's open end. The Flexipline's edge conforms to the Wave Generator's elliptical shape as the Generator rotates. The Flexipline's outer surface has teeth which contact the internal teeth of the Rigid Circular Spline, a rigid ring. The Flexipline has two fewer teeth than the Rigid Circular Spline. Thus, one revolution of the Wave Generator will cause relative motion between the Rigid Circular Spline and the Flexipline.

Suppose  $n_f$  is the number of teeth on the Flexipline, and  $n_r$  is the number of teeth on the Rigid Circular Spline. When the Rigid Circular Spline is held stationary, the reduction ratio,  $r$ , is determined by:

$$r = \frac{n_f}{n_f - n_r} \quad (1)$$

Note that since the Rigid Circular Spline has more teeth than the Flexipline, the ratio will be negative. This means that the Wave Generator and the Flexipline turn in opposite directions. When the Flexipline is held stationary, the Rigid Circular Spline is considered to be the output and rotates such that the reduction ratio,  $r$ , is determined by:

$$r = 1 - \frac{n_f}{n_f - n_r} \quad (2)$$

---

This research is partially supported by the National Science Foundation under contract number 8809088.

The ratio in this case is positive and the Rigid Circular Spline and Wave Generator rotate at the same direction. If  $n_f=400$ , and  $n_r=402$ , then equation 2 results in  $r=201$ . The analysis on this paper is for the latter case where the Flexipline is stationary and Rigid Circular Spline rotates the load. The holes in the Rigid Circular Spline fasten to the load.

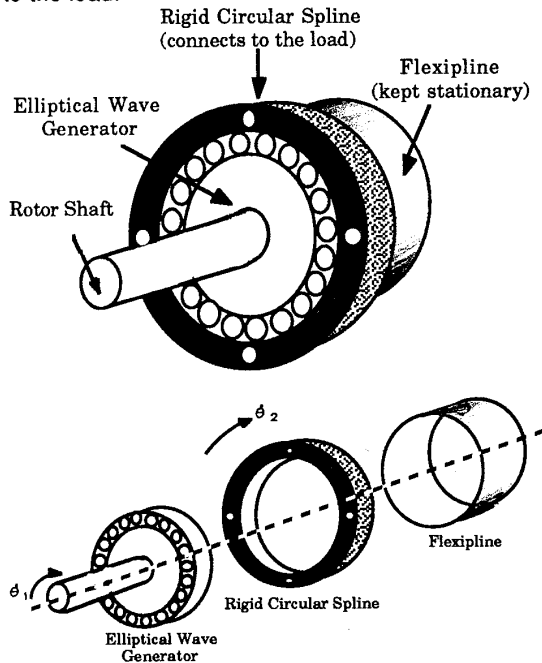


**Figure 1: Harmonic Drive Components. When the Flexipline is kept stationary, the Elliptical Wave Generator and the Rigid Circular Spline rotate at the same direction.**

### 3. Dynamic Behavior

This section describes the dynamic behavior of the harmonic drive. At this point no assumptions are made about the type of control employed for the motor that drives the Wave Generator. The Wave Generator is coupled directly to the motor shaft while the Flexipline is held stationary and the Rigid Circular Spline is employed to maneuver a load.  $U(s)$ , the voltage command to the motor amplifier, is the input.  $\theta_1(s)$ , the motor position (or the Wave Generator position), is the output. The transfer function  $G(s)$  represents the motor dynamics.

$$\theta_1(s) = G(s) U(s) \quad (3)$$

No assumptions on the structure or order of  $G^1$  are made at this point. The friction torque developed on the motor shaft by the Wave Generator bearing is assumed to be small. This assumption only simplifies our analysis; the friction forces can be added to the derivation later. Suppose the Rigid Circular Spline is employed to drive a load whose inertia is  $J_2$ . Inspection of Figure 2 results in the following equation for the dynamic behavior of the assembled Flexipline and the Rigid Circular Spline:

$$W - T = J_2 \ddot{\theta}_2 \quad (4)$$

$W$  is the torque that holds the Flexipline stationary.  $T$  is all possible external torques that oppose the motion of the Rigid Circular Spline (and its load).

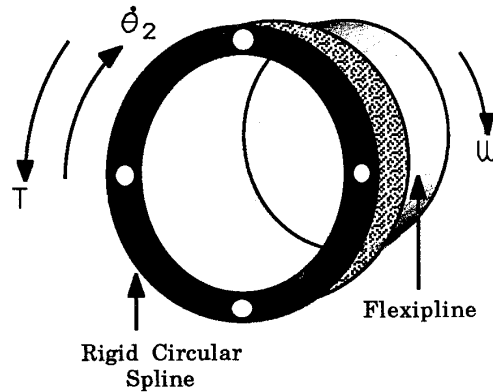


**Figure 2: The Circular Rigid Spline and the Flexipline. The Flexipline is held stationary and the Rigid Circular Spline rotates with a speed of  $\dot{\theta}_2$ .**

Assuming  $\dot{\theta}_1 = r \dot{\theta}_2$ , the block diagram of Figure 3 depicts one possible combination of equations 3 and 4 which can represent the dynamic behavior of the harmonic drive when maneuvering a load with inertia of  $J_2$ . Inspection of the block-diagram of Figure 3 shows that the torque that holds the flexipline,  $W$ , results from two independent variables: 1) the input voltage command to the amplifier input, 2) all torques that oppose the motion of the load. The block diagram of Figure 3 also depicts the non-backdrivability of the system where  $T$  does not affect  $\theta_2$ ; it only adds to  $W$ .

<sup>1</sup> The Laplace argument of various variables,  $s$ , are given only when the variables are introduced for the first time.

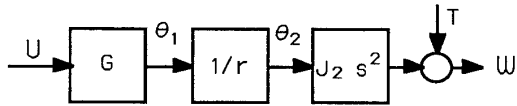


**Figure 3: The Dynamic Behavior of The Harmonic Drive Maneuvering a Mass With Moment of Inertia of  $J_2$ .**

If the Rigid Circular Spline and load with inertia  $J_2$  were in contact with an environment with stiffness and damping of  $K_2$  and  $C_2$ , the block diagram of Figure 3 should be modified as given in Figure 4 where  $E(s) = J_2 s^2 + C_2 s + K_2$ . Note that E can be any arbitrary dynamics representing the dynamics of the Rigid Circular Spline and its interacting environment. In particular we are interested in powered hand controllers for telerobotic applications where a human is in contact with a stick driven by a Rigid Circular Spline. (Section 6 will give a more detailed description about the hand controller).  $K_2$ ,  $C_2$  and  $J_2$  in the case of a hand controller represent the dynamic behavior of the human hand and the stick as seen from the Rigid Circular Spline. See reference [3] for an example in measurement of E for the human arm.

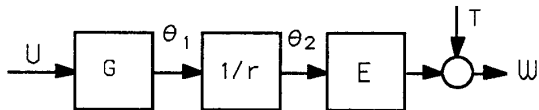


**Figure 4: The General Representation of the Dynamic Behavior of The Harmonic Drive when Rigid Circular Spline interacts with the Environment E**

#### 4. Instrumentation and Control

Our primary purpose is to develop an instrumentation which allows a designer to modify arbitrarily the behavior of the harmonic drive so it responds to the external torques T and becomes backdrivable. We suggest that W, the torque that holds the Flexipline stationary, be measured by installing four strain gages on either the Flexipline or the structure that holds the Flexipline. Since the Flexipline is stationary, the measurement of W is rather straightforward. This torque, after modification by a controller, is then used to drive the motor in the direction of T. Measuring joint torque on a rotating shaft in robotic systems has always been difficult for engineers. This design allows measurement of joint torques from a stationary part, the Flexipline cup.

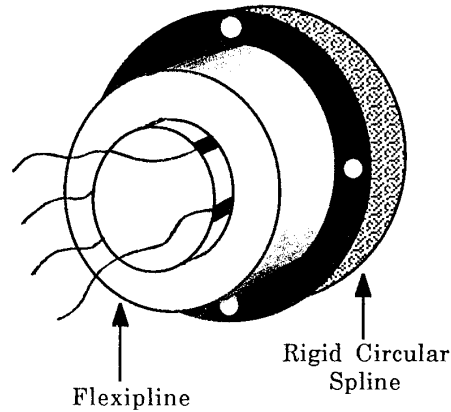


**Figure 5: Four strain gages on the Flexipline support measures W.**

Figure 6 shows the control architecture where the measured torque W is used to drive the motor after compensation by  $H(s)$ , and  $R(s)$  is the input command.

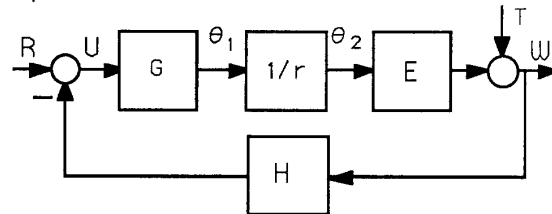


**Figure 6: The torque keeping the Flexipline stationary is used as a feedback to make the system backdrivable.**

Inspection of Figure 6 results in the following equation for  $\theta_2$ .

$$\theta_2 = P(s)R - S(s)T \quad (5)$$

where the transfer function P and S are given as:

$$P = \frac{\frac{G}{r}}{1 + \frac{GHE}{r}} \quad (6)$$

$$S = \frac{\frac{GH}{r}}{1 + \frac{GHE}{r}} \quad (7)$$

S is defined as the system *sensitivity transfer function* (1/impedance). Designers can shape the sensitivity transfer function via selection of a proper H. Inspection of equations 5, 6 and 7 reveals that when H is small, T does not affect  $\theta_2$ ,

the output motion, because  $S$  approaches zero. The system is therefore non-backdrivable. When  $H$  becomes very large (i.e., approaches infinity) over a finite frequency range, then  $P$  approaches zero and  $\theta_2$  from equation 5 will be a function of  $T$  only:

$$\theta_2 = -\frac{1}{E} T \quad (8)$$

If the system is carrying inertia  $J_2$  only, then  $E = J_2 s^2$  and equation 8 results in:

$$\theta_2 = -\frac{1}{J_2 s^2} T \quad (9)$$

Equation 9 resembles the Newton's Law for the inertia  $J_2$  under the torque of  $T$ . This means that for large values of  $H$ , the system will become totally backdrivable and responds to external torques as if there was no harmonic drive in the system. One cannot choose an arbitrarily large value for  $H$ ; the closed-loop stability of the system shown in Figure 6 must be guaranteed.

## 5. Stability and Performance

Before we discuss our goal in selection of  $H$ , it is important to bring up the limitations that have evolved from the block diagram of Figure 6:

1) If the system carries a mass only, then  $E = J_2 s^2$ . The term  $J_2 s^2$  in the loop gain of Figure 6 implies two zeros at the origin. If  $G$  has an integrator, the pole/zero cancellation at the origin results in an uncontrollable unstable mode. It is recommended that  $G$  be free of integrators. Motors with closed-loop positioning controllers do not have free integrators and result in constant DC values. The above discussion is also valid for  $H$ :  $H$  must not have any integrator. Any integrator of  $H$  will cancel the zeros associated with  $J_2 s^2$  resulting in an uncontrollable unstable mode.

2) Even when a  $G$  without integrators is considered for the system, the zeros at the origin do not let one choose a large value for  $H$ . This is true because term  $J_2 s^2$  results in a non-minimum phase loop transfer function. The large values for  $H$  drive the closed-loop poles to the zeros at the origin.

Note that the reason we are interested in the case of  $E = J_2 s^2$  is due to the fact that we believe the system of motor-harmonic drive must remain stable in its simplest form of functioning: carrying a mass with inertia of  $J_2$ . This inertia is at least equal to the inertia of the Rigid Circular

Spline. The more elaborate case is when the link connected to Rigid Circular Spline interacts with an environment.

The goal is to shape the sensitivity transfer function,  $S$ , within a bounded frequency range via the selection of a proper  $H$ . Suppose one wishes to choose  $H$  such that  $S$  becomes equal to a desired transfer function,  $G_d(s)$ , for a bounded frequency range. See Reference [6] for some suggestions on selection of  $G_d$ . Because  $\frac{GHE}{r}$  is very small due to the large value of  $r$ , equation 7 can be simplified to the following equation:

$$S = \frac{GH}{r} \quad (10)$$

The term  $\frac{GHE}{r}$  becomes even smaller at low frequencies in the case of  $E = J_2 s^2$ .  $G$  is the closed-loop transfer function of the motor and is constant within its bandwidth. In fact, a good closed-loop position controller yields a  $G$  with unity gain within its bandwidth: the system input and output are equal within the closed-loop bandwidth. Since shaping the system sensitivity function,  $S$ , makes sense only within the system bandwidth, we suggest that the DC gain of  $G$ , (referred to as  $G_0$ ) be used in equation 10. Equating the right hand side of equation 10 with a desired dynamics,  $G_d$ , leads to the following equation for  $H$ .

$$H = \frac{r}{G_0} G_d \quad (11)$$

Note that equality 11 does not guarantee the system closed-loop stability; it is only a guideline for practitioners to choose  $H$ . According to equation 11, within the bandwidth of  $G$ ,  $H$  has the same structure of  $G_d$  scaled by  $r/G_0$ . This choice of  $H$  must also guarantee the closed-loop stability; if the system is not stable for a choice of  $G_d$ , then one must choose a smaller  $G_d$  for the desired sensitivity function [2, 4, 5].

## 6. Experiments

A set of experiment was carried out on an active one-degree-of-freedom hand controller at the Motion Control Laboratory of the University of Minnesota (Figure 7)<sup>2</sup>. Hand controllers are

<sup>2</sup> The hardware for construction of this hand controller was donated by CIMCORP located in Shoreview, Minnesota. The author appreciates this generosity.

powered joysticks that can be used by pilots. Hand controllers can also be used as master robots in telerobotic systems when rate-control governs the dynamics of the master robot. Another application for hand controllers can be found in maneuvering unmanned underwater vehicles where the operator maneuvers the vehicle from a mother ship using a hand controller. Traditionally, the speed of the underwater vehicle in various directions is a function of the position of the hand controller in various directions. The hand controller's range of motion usually is small: on the order of two-inch translational motion and  $\pm 10^\circ$  rotational motion.

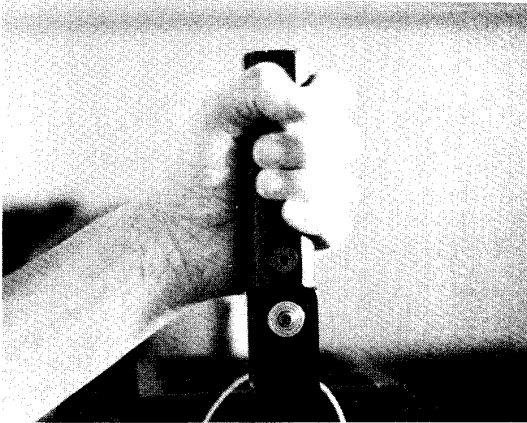


**Figure 7: Hand Controller**

A closed-loop positioning controller was designed for the motor such that the widest bandwidth is achieved for  $G$  while the motor remains robust in the presence of its unmodeled dynamics.  $G$  is given by equation 12 resulting in approximate bandwidth of 2 rad/sec.

$$G = \frac{125892.5}{s(s^2 + 140s + 4900) + 125892.5} \frac{\text{rad}}{\text{rad}} \quad (12)$$

The inertia seen by the Rigid Circular Spline is  $J_2 = 1.1534 \text{ slug}\cdot\text{ft}^2$  and  $r=201$ . It is desired that the system exhibits a sensitivity of 1 degree/lbf-ft (or 0.01745 rad/lbf-ft) for widest possible bandwidth. In other words for every one lbf-ft exerted by a pilot, the stick should move 1 degree. This resembles the dynamic behavior of a spring.  $G_o$  is unity within the bandwidth of  $G$  (about 2 rad/sec); therefore, from equation 11  $H = 201 \cdot 0.01745 = 3.507 \text{ rad/lbf-ft}$ . A set of experiments were carried out to demonstrate that the ratio of the stick motion,  $\theta_2$ , over the imposed

torque,  $T$ , is in fact 1 degree/lbf-ft. Figures 8 shows the torque that the pilot imposed on the stick. The pilot first pulls about 4 lbf-ft and then pushes about 4 lbf-ft. Figure 9 represents the stick motion. Inspection of Figures 8 and 9 shows that steady state torque of  $\pm 4 \text{ lbf-ft}$  results in  $\pm 4$  degree motion in the stick.

In another set of experiments, the pilot maneuvers the stick with a higher frequencies; Figure 10 shows the torque imposed by the pilot on the stick. Figure 11 shows the stick motion. It can be observed that the ratio of the stick position over the pilot torque for the first five seconds of the experiment is about 1 degree/lbf-ft while this ratio has been attenuated for the second five seconds of the experiment. This experiment shows that the target dynamics has been achieved only within the bandwidth of  $G$  only.

## 7. Conclusion

This article describes how a harmonic drive can be instrumented with force sensor to develop backdrivability. We have framed the harmonic drive backdrivability via a sensitivity transfer function. The sensitivity transfer function is defined as the transfer function that maps the external forces to the harmonic drive output position. It is shown that one cannot shape arbitrarily the system sensitivity function of a DC motor-harmonic drive. The larger the desired sensitivity transfer function,  $G_d$ , (i.e. more backdrivability), the smaller the stability range.

## 8. References

- 1) de Silva, C. W., *Control, Sensors, and Actuators*, Prentice-Hall, Cliffs, NJ, 1989.
- 2) Kazerooni, H., "On the Robot Compliant Motion Control", *ASME Journal of Dynamic Systems, Measurements, and Control*, Vol. 111, No. 3, Sep. 1989.
- 3) Kazerooni, H., "Human-Robot Interaction via the Transfer of Power and Information Signals", *IEEE Transactions on Systems and Cybernetics*, Vol. 20, No. 2, Mar. 1990.
- 4) Kazerooni, H., "On the Contact Instability of the Robots When Constrained by Rigid Environments," *IEEE Transactions on Automatic Control*, Volume 35, Number 6, June 1990.
- 5) Hogan, N. "Impedance Control: An Approach to Manipulation," *ASME Journal of Dynamic Systems, Measurement, and Control*, Vol. 107, No. 1, pp. 1-24, March 1985.
- 6) Kazerooni, Sheridan, T. B., Houpt, P. K., "Fundamentals of Robust Compliant Motion

for Manipulators," *IEEE Journal of Robotics and Automation*, Vol. 2, No. 2, June 1986.

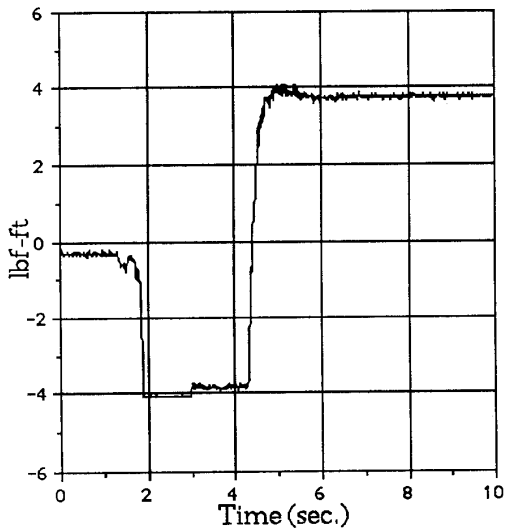


Figure 8: The Torque Imposed by the Pilot on the Hand controller

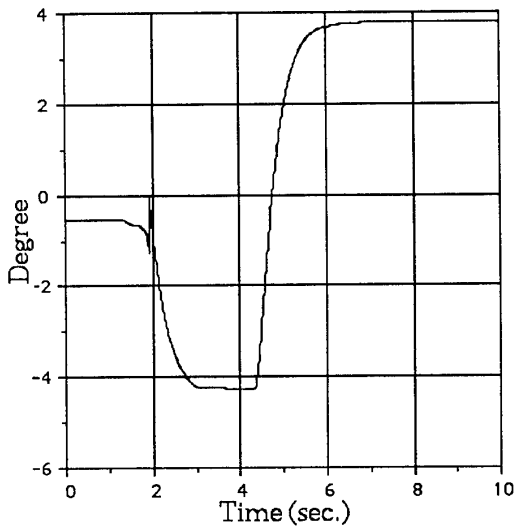


Figure 9: The Position of the Hand controller

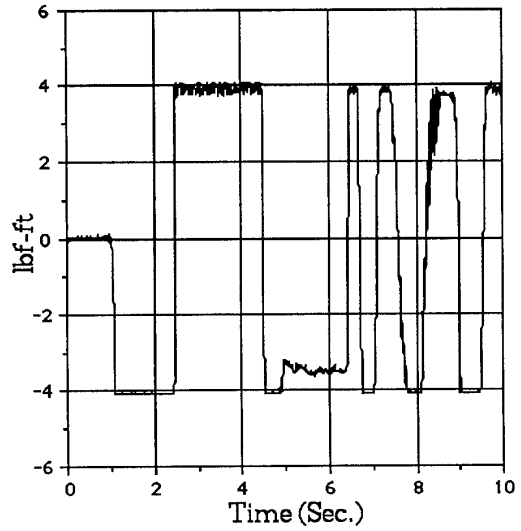


Figure 10: The Torque Imposed by the Pilot on the Hand controller

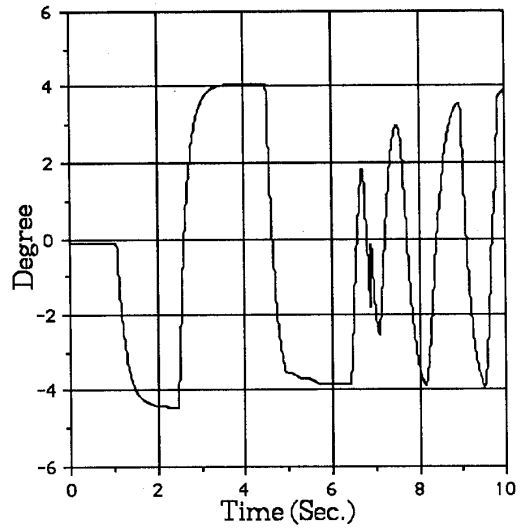


Figure 11: The position of the hand controller is proportional with the imposed torque only at low frequencies.